Article

Rapid Identification of Foodborne Pathogens in Limited Resources Settings Using a Handheld Raman Spectroscopy Device

Cid Ramon Gonzalez-Gonzalez [1], Mark Hansen [2,†] and Alexandros Ch. Stratakos [3,*,†]

1   Department of Biochemistry Engineering, Tecnológico Nacional de México Campus Acayucan, Acayucan 96100, Mexico
2   Centre for Machine Vision, Bristol Robotics Lab, College of Arts, Technology and Environment, University of the West of England, Bristol BS16 1QY, UK
3   Centre for Research in Biosciences, College of Health, Science and Society, University of the West of England, Bristol BS16 1QY, UK
*   Correspondence: alexandros.stratakos@uwe.ac.uk; Tel.: +44-(0)-11732847-43
†   Mark Hansen and Alexandros Ch. Stratakos jointly directed this work.

Featured Application: Here, we report a practical and precise method for the identification of foodborne pathogenic bacteria using a Raman handheld device equipped with an orbital raster scan (ORS) technology that enables the system to generate a distinct fingerprint of bacteria suspended in media broth by applying principal component analysis (PCA) and support vector machine (SVM) as classifiers. This system relies on isolation from the source to ensure the generation of fingerprints of axenic cultures. It requires very little sample preparation and is significantly less costly than other Raman technologies. Thus, this system could be easily implemented in limited-resource settings.

Abstract: Rapid and precise methods to detect pathogens are paramount in ensuring food safety and selecting appropriate disinfection treatments. Raman spectrometry is a promising technology being investigated for detecting pathogens and achieving rapid, culture-free, and label-free methods. Nonetheless, previous Raman techniques require additional steps, including the preparation of slides that could introduce significant variability. In this study, we investigated the capability of a Raman handheld device for rapid identification of monocultures of *Listeria monocytogenes*, *Salmonella* Typhimurium, *Escherichia coli* O157:H7, and *Staphylococcus aureus*, and the combination of co-cultures in BHI broth suspension by utilising principal component analysis (PCA) and support vector machine (SVM) classification of Raman spectra. The detection method accurately identified monocultures (0.93 ± 0.20), achieving good discrimination after 24 h of bacterial growth. However, the PCA–SVM system was less accurate for classifying co-cultures (0.67 ± 0.35). These results show that this method requires an isolation step followed by biomass enrichment ($>8 \log_{10}$ CFU/mL) for accurate identification. The advantage of this technology is its simplicity and low-cost preparation, achieving high accuracy in monocultures in a shorter time than conventional culture-dependent methods.

Keywords: portable Raman; rapid identification; foodborne pathogens; limited-resource settings

1. Introduction

Foodborne pathogens are a severe problem for the agri-food industry and a serious concern for public health on a global scale. The cost is divided between social aspects such as medical care, reduction in quality of life, mortality, and the agri-food industry, i.e., costs for regulation compliance, product recalls, and tracing back-contamination [1]. Specific bacterial pathogens may cause severe illness or even become life-threatening within a few days. Currently, among the most critical bacterial agents are *Listeria* (*L.*) *monocytogenes*,

Salmonella spp., and the Shiga toxin-producing *Escherichia* (*E.*) *coli* O157 [2]. *L. monocytogenes* is a Gram-positive, biofilm-forming, and ubiquitous microorganism that can grow at low temperatures, making it a serious health risk for the food industry. Moreover, listeriosis may induce abortion in pregnant women, showing a high mortality rate of about 13 to 34% [3]. It is estimated that listeriosis-related costs reach up to £245 million per year in the UK [3]. *Salmonella* spp. cause acute gastroenteritis and are considered the leading cause of morbidity and mortality in developed and developing countries [4]. There are continuous increases in cases of salmonellosis in the EU related to the consumption of contaminated poultry [5]. *E. coli* O157:H7 is a Shiga-toxin-producing pathogen (STEC) that may cause acute diarrhoea and severe kidney damage. Serotype O157 was associated with the most reported infection incidences in the EU in 2017 [6]. Moreover, methicillin-resistant *Staphylococcus* (*S.*) *aureus* (MRSA) strains are of particular interest. They can cause severe infections in humans and animals and have shown resistance to other antimicrobial groups, raising serious concerns. Its transmission has been associated with community interaction, healthcare (i.e., in hospitals), and livestock (zoonosis) [6]. Therefore, rapid identification of pathogenic bacteria in food is paramount to making decisions in time. Selective culture followed by biochemical identification is used in conventional laboratories for identification. However, this path can take up to 6 days to complete [7]. Other methods provide more rapid and accurate identification, including PCR, serological, and surface protein identification using matrix-assisted laser desorption ionisation–time of flight (MALDI–TOF) mass spectrometry [8]. However, these methods generally require the acquisition of high-cost equipment and reagents.

Raman spectroscopy (RS) is a non-invasive and non-destructive spectroscopic technique based on the molecular vibrations derived from the interaction of photons from a laser source when they hit the molecules of a substance characterised by specific chemical groups [9]. It has the advantage that it can probe numerous biochemical compounds on the cell surface without needing a particular marker [10]. However, only 1 in 10^6–10^8 scattered photons correspond to Raman scattering phenomena, producing a weak signal. Therefore, in addition to mathematical signal-to-noise data amplification by computational models, other techniques have been developed to increase Raman efficiency. For instance, surface-enhanced Raman scattering (SERS) significantly upturns Raman scattering efficiency, up to 10^6 times, compared to conventional Raman [11]. This consists of using metallic particles such as silver or gold as substrates that interact with the target molecules, increasing their signal intensity [10]. SERS has been reported to detect *E. coli* on grounded beef within three hours [12] (p. 171) and *Pseudomonas* from drinking water within 15 min of analysis time [13]. This promising technique allows for the rapid identification of culture-free and label-free microorganisms. Nevertheless, SERS requires expensive equipment and infrastructure, making it impractical for laboratories in limited-resource settings. Moreover, its applicability depends on the affinity of the target compound for metal surfaces to provide an adequate signal, and the standardisation of substrates is necessary to achieve reproducible results [10,14].

RS coupled to confocal microscopy can interrogate a single cell for components, increasing the accuracy of cell classification [15]. This technique and convolutional neural networks (CNN) have been reported to classify bacterial cells of clinical importance, such as *L. monocytogenes*, *Salmonella*, and *S. aureus*, achieving rapid and culture-free identification with high accuracy [15]. Its limitation is that the slide and sample preparation process may introduce high variability between laboratories as no standardised condition consensus exists. These factors include media type, centrifugation conditions, slide drying, and the age of the slide preparation [16].

Handheld Raman devices can scan samples in situ, achieving high accuracy. Farber and Kurouski (2018) reported a Raman handheld device technique to identify plant pathogens on maize kernels, discriminating with high accuracy (100%) between healthy and infected kernels [17]. The advantage of using portable devices is their practicality and ability to test in situ. In the present study, we tested a portable handheld Raman device

with the capability of screening a large area to obtain a single fingerprint in liquid-phase suspension. No reports have been made using a portable Raman device with this technology to identify bacteria. Thus, this study aimed to develop a detection method using a Raman handheld spectrometer to identify high-threat foodborne pathogenic bacteria in liquid cultures, suitable for limited-resource settings.

2. Materials and Methods

2.1. Material and Strains

The bacterial strains used in this study were provided by the Department of Applied Sciences at the University of the West of England. *L. monocytogenes* ATCC® 35152 (NCTC 7973), *Salmonella enterica* serotype Typhimurium ATCC® 14028, *Staphylococcus aureus* ATCC® 25923 (NCTC 12981), and *E. coli* ATCC® 25922 were activated from a frozen culture in brain heart infusion broth (BHI, Oxoid®, *Oxoid*, UK) and incubated at 37 °C. An aliquot of BHI overnight culture was then streaked onto trypticase soy agar (TSA, Oxoid®), incubated overnight (37 °C), and then maintained as fresh colonies for up to a week under refrigeration (2–4 °C). For the experiment, single colonies were inoculated in BHI broth in triplicate for 24 h to reach the stationary growth phase. Serial dilutions were made using BHI broth and reinoculated in the same media (10 mL) to obtain an initial cell concentration of 10 CFU mL^{-1}. Inoculated media tubes were incubated at 37 °C under agitation at 100 rpm. Cell counting for growth kinetics and Raman readings were determined at 0, 2, 4, 6, 8, 18, and 24 h. BHI media without inoculum treated under the same temperature conditions was used as a negative control for cell counting and Raman readings. The growth rate (μ) was calculated as the slope of the following Equation (1):

$$\ln x = \mu \times t + \ln x_o \tag{1}$$

where μ is the growth rate (h^{-1}), x is the biomass (cell mL^{-1}), t is time (h) during the log phase, and x_o is the biomass at the initial time.

2.2. Cocultures

Two different combinations of cultures were studied, namely, *L. monocytogenes–S. aureus* and *L. monocytogenes–S. enterica*, to determine the level of discrimination that a Raman signal can provide for combined bacterial strains compared to the level of discrimination in monocultures inoculated in BHI. To distinguish between cells, differential media was used as follows: Oxoid Chromogenic Listeria agar (OCLA, Oxoid®) supplemented with Oxford formulation Listeria selective supplement (Oxoid®) and Brilliance Listeria differential media (Oxoid®) for *L. monocytogenes*; Oxoid Baird-Parker agar base (Oxoid®) with RPF Supplement SR0122 (Oxoid®) for *S. aureus*; and xylose–lysine–desoxycholate Agar (XLD, Oxoid®) for *S. enterica*. Cell counting was determined by plating out serial dilutions using maximum recovery diluent (Oxoid®) on differential media.

2.3. Raman Measurements

Raman signals were determined using a Mira M-1 handheld device (Metrohm NIRSystems ®, Herisau, Switzerland). The system is equipped with a 768 nm laser with a wavenumber range of 400–2300 cm^{-1} and a spectral resolution of 12–14 cm^{-1} (FWHM) across the whole range, with an output power of ≤100 mW. The equipment uses an orbital raster scan (ORS) as a detection technique that allows for interrogation of a large area over the sample. A 1 mL sample was taken into a clear glass vial (Thermofisher Scientific, Swindon, UK) and placed into the device's vial holder. Five readings were carried out for each replicate (*n* = 3). The acquisition time was 4.5 s. The first reading was taken out as it showed a significantly different spectrum than the rest (data not shown). We ensured that the vial was properly clean before proceeding (i.e., no protein residues or fingerprints). The data were collected and transformed for data analysis using Mira Cal® software version 1.2 for Microsoft Windows®.

2.4. Data Analysis and Statistics

2.4.1. Data Format

Each replicate's spectrum was stored in its file in ASCII format, in which each line consisted of the wavenumber and the response separated by a tab character. This was the data used for our classification experiments, i.e., no normalisation or background subtraction was performed to keep the processing as direct as possible.

2.4.2. Data Analysis

The classification was performed using a Support Vector Machine-based classifier. This approach seeks one or more hyperplanes that define a boundary (maximum margin) that separates classes. Our implementation was based on the Python library scikit-learn (1.0.2), with a regularisation parameter of 20 and the default radial basis function kernel. A 5-fold cross-validation paradigm was used to validate the SVM by randomly selecting a validation fold five times, training the SVM on the remaining data, and then validating the data on the validation fold (that the SVM had not been trained on). The classification was then performed by assigning a class based on the location and distance to the hyperplane.

As shown in Figure 1, the raw Raman data were smoothed by fitting a cubic B-spline to identify peaks. A continuous wavelet transform (CWT), well suited to finding sharp peaks in noisy data, was then used to identify peaks using a window width of 12.5 (empirically determined). Whilst this method gave satisfactory results for visually inspecting the spectra, it was sensitive to the selected parameters. These peaks are shown in Figure 1 as blue dots.
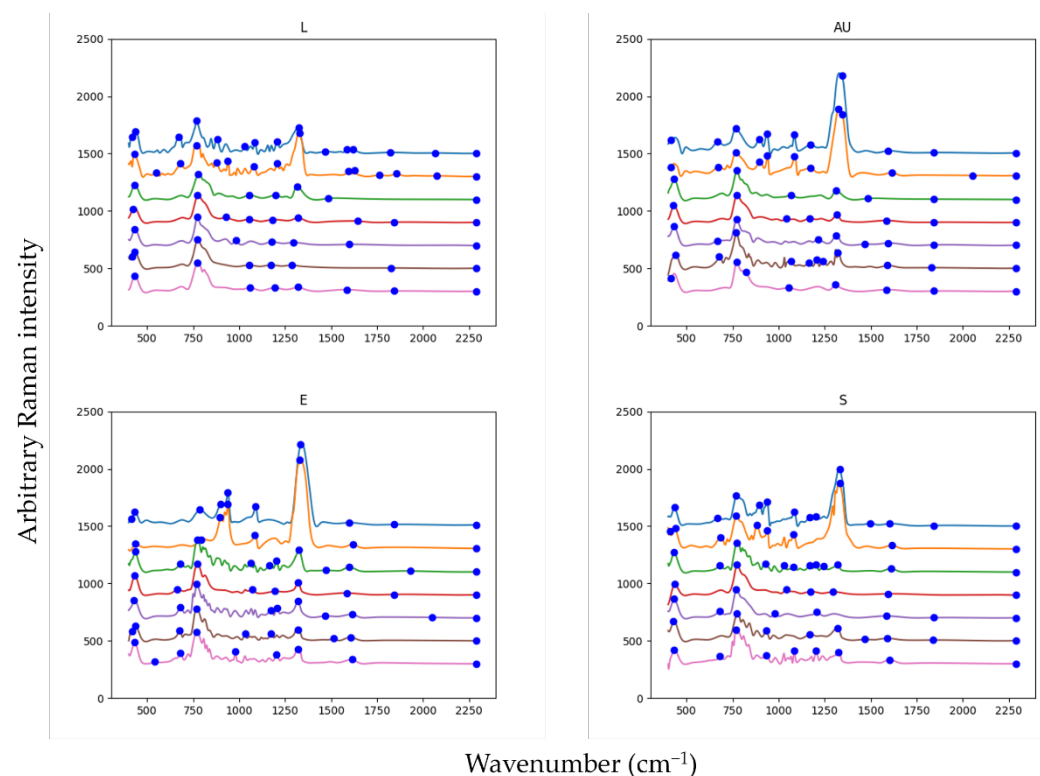
Figure 1. Raman spectra for each monoculture: *L. monocytogenes* (L), *S. aureus* (AU), *E. coli* (E), and *S. enterica* (S); lines are displayed for better observation and represent the spectra acquired at different time points from top to bottom: 24 (blue), 18 (orange), 8 (green), 6 (red), 4 (purple), 2 (brown), and 0 h (pink).

3. Results

3.1. Pathogen Identification in Monocultures

Our first approach was to investigate the capability of Raman spectroscopy to detect a discriminatory signal between species to identify them as early as possible within 24 h of

bacterial growth in BHI broth. We used this media as it is rich in nutrients and allows the growth of various fastidious microorganisms; therefore, it can be used as standard media. Figure 1 shows that signals increased in intensity after 18 h and 24 h of growth compared to spectra found at 8 h or earlier. This indicates that more distinctive and intense signals were achieved after 18 h of growth at 37 °C, offering a better signal-to-noise ratio. The same was observed for all the strains tested, significantly *E. coli* and *S. aureus.*

Noticeably, signals for *L. monocytogenes* were weaker than the other strains. This correlates to *Listeria's* lower growth rate than the other monocultures (Table 1). Indeed, *Listeria's* Log CFU mL^{-1} was significantly lower when cocultured with *S. aureus* and *S. enterica* (Figure 2).

Table 1. Growth kinetics of *Listeria monocytogenes*, *Salmonella* v. Typhi, *E. coli* O157:H7, and *S. aureus* in monoculture, and *Listeria + Salmonella* in coculture (x) and *Listeria + S. aureus* in coculture (y). Results are expressed as the mean (*n* = 3) ± SD of Log CFUmL^{-1}.

Strain	Monocultures								Coculture (x)				Coculture (y)			
	Listeria		*Salmonella*		*E. coli*		*S. aureus*		*Listeria x*		*Salmonella x*		*Listeria y*		*S. aureus y*	
μmax (h^{-1})	0.96		1.83		1.71		2.05		0.85		1.83		1.02		1.73	
Time	Mean	SD	Mean	SD	Mean	SD	Mean	SD	Mean	SD	Mean	SD	Mean	SD	Mean	SD
0	1.57	0.24	1.63	0.72	2.06	0.49	1.12	0.10	<0.10	0.00	1.75	0.06	0.86	0.09	0.59	0.26
2	2.28	0.08	2.19	0.23	2.38	0.20	1.70	0.07	0.45	0.54	2.64	0.12	1.83	0.06	1.89	0.08
4	3.03	0.22	4.07	0.14	3.96	0.25	3.75	0.09	0.87	0.81	4.51	0.03	2.78	0.08	3.84	0.14
6	3.89	0.14	5.91	0.02	5.81	0.06	5.63	0.02	2.13	0.30	6.23	0.12	3.65	0.16	5.17	0.05
8	4.92	0.02	7.73	0.04	7.76	0.04	7.02	0.05	2.86	0.22	7.89	0.05	4.37	0.09	6.48	0.10
18	9.50	0.12	9.07	0.04	9.46	0.10	9.42	0.15	5.10	0.17	8.88	0.01	7.39	0.09	9.30	0.08
24	9.55	0.09	8.98	0.07	9.45	0.05	9.42	0.14	5.73	0.38	9.09	0.18	7.65	0.16	9.39	0.14
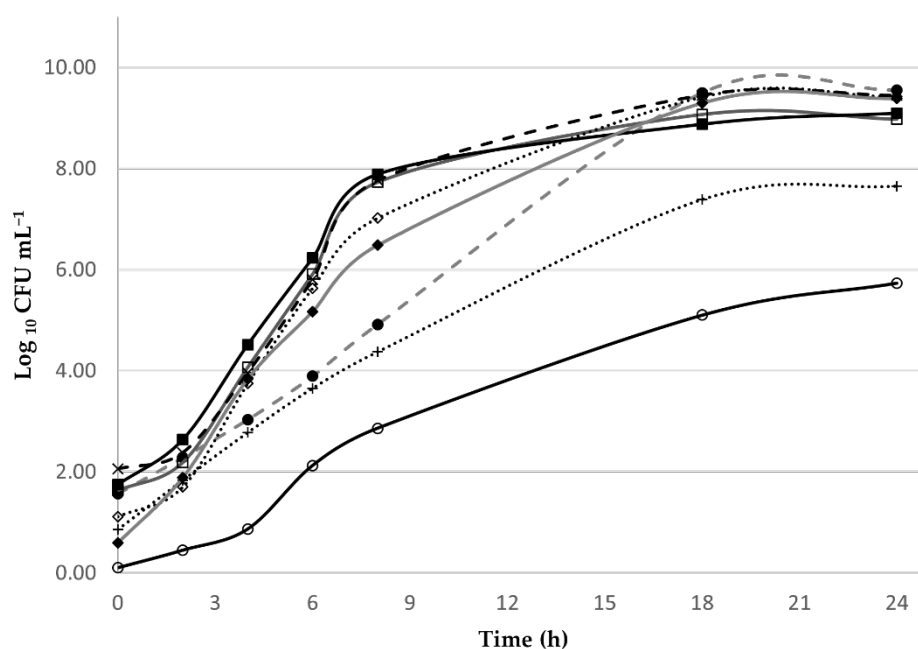
Figure 2. Growth kinetics of monocultures: *L. monocytogenes* (dashed grey ●), *S. enterica* (grey □), *E. coli* (dashed black ✕), *S. aureus* (dotted black ◇); cocultures: *L. monocytogenes* (x) (black ○), *S. enterica* (x) (black ■); *L. monocytogenes* (y) (dotted black +), and *S. aureus* (y) (grey ◆).

Results from the 5-fold validation show that SVM can identify the difference between the monoculture samples. Confusion matrices presented in Figure 3 show the actual and predicted classes for the 5-fold cross-validation. Correct predictions follow the diagonal, and incorrect predictions can then be seen in the other cells of the matrix. The output at 24 h gave the best response to discriminate between the bacterial spectra with the highest accuracy. In Figure 3, SMV results for the 5-fold cross-validation after 24 h showed an

accuracy of 0.93 (±0.20) predicting the right strain, whereas 18 h and 8 h showed accuracies of 0.88 (±0.27) and 0.46 (±0.10), respectively. This positive correlation among accuracy, time, and cell growth is related to the increase in the intensity of Raman signals and the rise of metabolites concentration achieved at the stationary growth phase. Moreover, at 24 h, SVM predicted *E. coli* and *L. monocytogenes* with high accuracy (≈1) but predicted, with a marginal error, *S. enterica* with 0.81 and *S. aureus* with 0.89 accuracies. In addition, the error increased 0.33 times for *L. monocytogenes* prediction, misleading prediction to *S. enterica* at 18 h of growth.
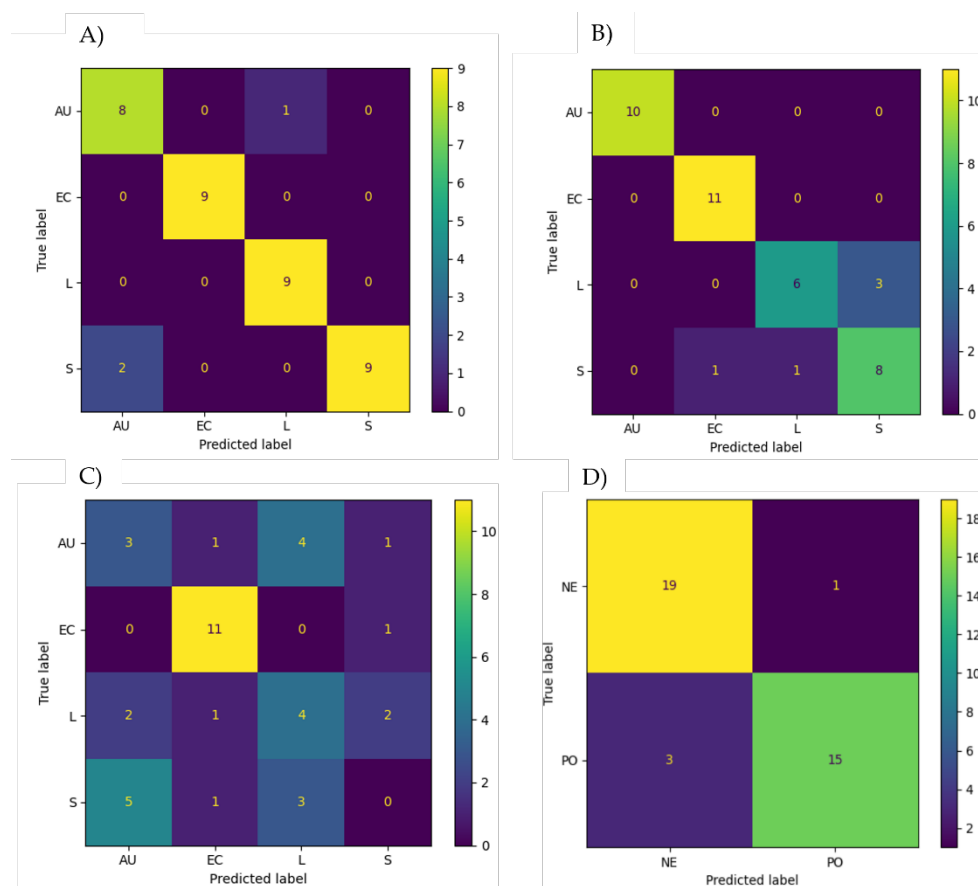
Figure 3. Confusion matrices of SVM 5-fold cross-validation for monocultures: *S. aureus* (AU), *E. coli* (EC), *L. monocytogenes* (L), and *S. enterica* (S); at three different times: (**A**) 24, (**B**) 18, and (**C**) 8 h; (**D**) confusion matrix of SVM 5-fold cross-validation for Gram-positive (PO)/Gram-negative (NE) at 24 h. Higher numbers show a stronger correlation between the predicted and the actual label.

3.2. Gram Classification

Raman spectroscopy was evaluated as a means of Gram bacteria classification. The 5-fold cross-validation distinguished Gram-positive (*L. monocytogenes* and *S. aureus*) and Gram-negative (*S. enterica* and *E. coli*) strains at 24 h with high accuracy (0.89), as shown in Figure 3D. The main structural difference between Gram-positive and Gram-negative bacteria is the presence of peptidoglycans on the cell wall. This was observed by Lemma et al. (2016), reporting high-intensity peaks at 497 cm^{-1} attributed to polysaccharides of the Gram-positive bacteria cells using SERS [18]. Another study did not report significant differences between Gram-positive or Gram-negative bacteria using SERS [19]. However, tip-enhanced Raman spectroscopy (TERS) can differentiate between Gram category bacteria in the 2800–3000 cm^{-1} region attributed to methylene stretching vibrations [20]. It is noteworthy to consider that the chemometrics signals may differ for each Raman technique [9]. As observed in Table 2, ORS Raman mainly provided signals distinctive to Gram-positive strains, at 1295–1297 cm^{-1} (CH_2 fatty acid deformation). Moreover, signals

of Gram-negative strains, at 1086–1087 cm^{-1} (DNA phosphate backbones), enabled the model to predict them accurately. Thus, this system could also classify bacteria at this level.

3.3. Pathogen Identification in Cocultures

To investigate the capability of RS to discriminate between bacteria in complex samples, we cocultured *L. monocytogenes* (Gram-positive) with *S. enterica* (Gram-negative) or *S. aureus* (Gram-positive). According to Figure 4, *Listeria* coculture with other strains did not contribute as much to the PCA signal intensity as *S. aureus* or *S. enterica*. This could be associated with the slower growth rate of *L. monocytogenes* compared to the other bacterial strains in coculture due to nutrient competition. This would explain why the coculture principal component was mixed with the neat clustering of monocultures in the plot of the three principal components in Figure 5B. The monocultures showed good clustering with no overlap between groups (Figure 5A). However, with the introduction of cocultures, the groupings were not so distinct and did not align with constituent monocultures. The source of this confounding effect was unknown, but it is hypothesised that the lower growth rate of *L. monocytogenes* means that the other pathogen in the co-culture dominates the signal. This is potentially supported by the clustering of the *S. enterica + L. monocytogenes* (brown) co-culture around the *S. enterica* (red) cluster and the *S. aureus + L. monocytogenes* (purple) around the *S. aureus* (green) cluster. We might expect that if the *L. monocytogenes* concentrations are equal to their partner culture, the resultant point would project into the space between the constituent mono-culture clusters.
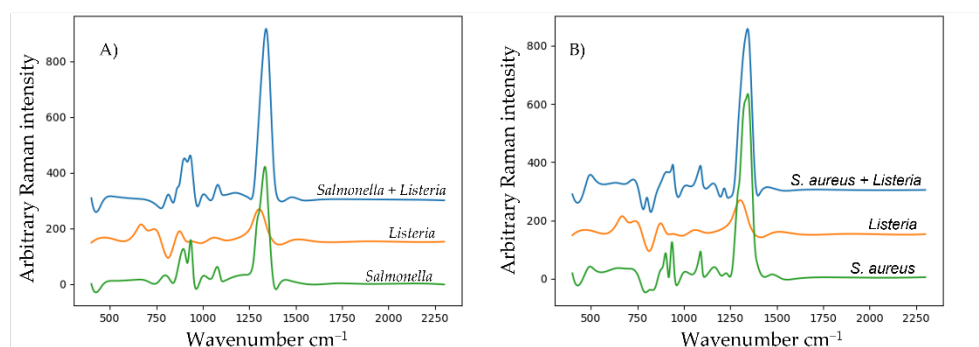
Figure 4. Comparison of control-subtracted Raman spectra (RS) of coculture mixtures and their corresponding monoculture RS components at 24 h: (**A**); *L. monocytogenes* and *S. enterica* coculture (top blue line), *L. monocytogenes* (orange line), and *S. enterica* (green line) and (**B**) *L. monocytogenes + S. aureus* coculture (top blue line), *L. monocytogenes* (orange line), and *S. aureus* (green line).
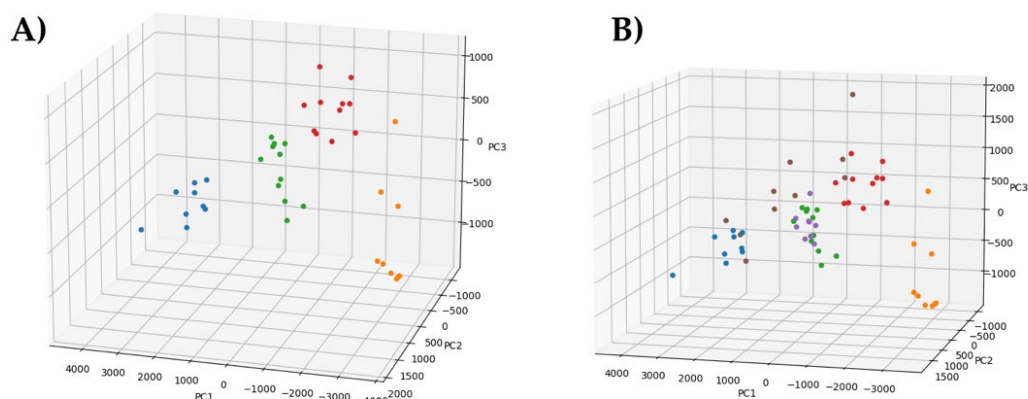
Figure 5. The three principal components explain ~60% of the variance for 24 h samples in (**A**) monocultures and (**B**) monocultures + cocultures. Code: *E. coli* (blue), *L. monocytogenes* (orange), *S. aureus* (green), *S. enterica* (red), *L. monocytogenes + S. aureus* (purple), *L. monocytogenes + S. enterica* (brown).

4. Discussion

Previous reports have used a chemometric approach to identify bacteria, especially those employing SERS technology coupled with microscopy interrogating single cells and specific cell wall areas [21,22]. Although assigning a signal to a particular compound is not always possible, this study compared the spectra acquired to previous reports using similar Raman technologies shown in Table 2. Each strain spectrum differed from the non-inoculated control, although some peaks are matched in all the samples at the Raman shift (cm^{-1}) axis. This is the case for signals at 424–427, 764–766, 804–806, 940–943, and 1333–1335 cm^{-1} Raman shift, indicating molecules existing in the media, such as carbohydrates (C-C and C-O-H) and proteins. Furthermore, some peaks were distinctive for each species, such as 618 (Phe) and 670 (Val) cm^{-1} shifts for *S. enterica*, 657 (Tyr), and 901 (teicuronic acid present in Gram-positive cell wall) cm^{-1} shifts for *S. aureus*. Interestingly, this last peak was not observed in *L. monocytogenes*, another Gram-positive strain, but in *S. enterica*, where the adenine signal can overlap. Instead, peaks in *L. monocytogenes* spectra appeared at 1000 (Phe), 1173 (C–H, wagging of Tyr, guanine, cytosine, fatty acids, CH$_3$ deformation), 1285 (amide III, CH$_2$ twisting), 1582 (guanine, adenine, ring stretching, Phe, Trp), and 1635 (thymine, guanine) cm^{-1} shifts. Interestingly, a prominent peak found at 1333 corresponds to amide III vibrations, Trp, and Cα-H vibrations, and CH-deformation is significantly enhanced after 18 h and 24 h for all the strains but not in control, indicating an increase of transmembrane proteins that characterise mature cells in the stationary growth phase [23].

Other signals could not be associated with other compounds in the literature but are distinctive of each sample, creating a particular fingerprint and allowing the discrimination between them. This is the case for two remarkable shifts noticed at 779 and 895 for *E. coli*. No compound was associated in previous reports with these specific shifts. However, these are distinctive peaks in the fingerprint of *E. coli* at 18 and 24 h of growth. The Raman handheld device used in this study is loaded with a 785 nm laser with Orbital Raster Scan (ORS) technology that enables the system to scan a larger area than conventional Raman, allowing the analysis of more complex structures [24]. Moreover, it has been suggested that the 785 nm wavelength falls within an optimum balance between a reasonable signal-to-noise ratio and low damage to the cell structure [25]. It was observed that shorter wavelength lasers provide spectra with less noise but increase cell degradation, whereas longer wavelengths lower Raman scattering efficiency [25]. However, the spectra acquired in this study are likely a composite of the molecules suspended in the media and those present on the bacterial cell surface. Hence, PCA and SVM classifier systems were used to identify the studied strains based on a unique fingerprint. The data analysis in this study was made directly without normalising data, subtracting the background as described in the methodology section. Future work will investigate the effects of adding a normalising pre-processing step, such as normalising the 1000 nm response to unit magnitude.

Previous studies have reported Raman techniques for rapidly detecting foodborne pathogenic bacteria. Ravindranath et al. (2011) described a method to distinguish between *S. enterica*, *E. coli*, and *S. aureus* simultaneously using a combination of nano-membranes with metallic nanoparticles loaded with pathogen-specific antibodies for SERS [26]. This technique accomplished rapid detection under 45 min with a detection limit of 10^2–10^3 CFU mL^{-1}. Another study reported the detection of *Vibrio parahaemolyticus* as low as 10 CFU mL^{-1}, building highly selective aptamers with golden nanoparticles and cyanine dye 3 (Cy3) using the SERS approach on seafood samples [27]. A low detection limit is one of the main advantages of SERS and Raman micro-spectroscopy due to its ability to interrogate one single cell and a relatively short preparation time. Thus, these techniques only isolate cells from clinical or food processing samples [10]. Alternatively, the ORS system used in this study for pathogen detection depends on high concentrations of cells at the stationary phase of growth after 24 h, when the strongest signal is found. Concentration techniques such as centrifugation and resuspension can be used; however, due to its high sensitivity, the Raman signal may change significantly when the cells are in

starvation [28]. Previous studies have effectively used a Raman handheld device equipped with an ORS system to test the authenticity of parmesan Reggiano cheese, showing good performance in predicting authentic parmesan cheese from non-authentic parmesan cheese by acquiring the spectra directly from packaged grated samples [29]. The same technology is reported in the present study; using the cell suspension in BHI broth does not require further preparation, such as the fixation on costly slides or other separation steps. Then the preparation time is reduced to media preparation and cell growth, as it requires colony isolation followed by a subculture in broth media. Furthermore, the portability of the Raman handheld allows measurements to be taken in situ, using less space and very few steps of preparation, such as making dilutions. Given that the Raman scanning system relies on the ORS to average the signal spectrum of several cells on suspension, it is essential to assure an axenic subculture in the media broth to guarantee the spectra's homogeneity.

Table 2. Peak positions and tentative attributions for Raman spectra of control media broth BHI, *Listeria*, *S. aureus*, *E. coli*, and *Salmonella* based on similar studies [25,29–35]. Distinctive peaks for each strain or control are coloured in green, peaks matching Gram-positive are coloured in blue, Gram-negative are coloured in red, and bolded signals match with all the samples, including controls. Data are expressed in cm^{-1}; spectral resolution: 12–14 cm^{-1}.

Control BHI	*Listeria*	*S. aureus*	*E. coli*	*Salmonella*	Attribution
424	**426**	**426**	**427**	**426**	
				434	
437	437				
446					
			449		
	454				
		497			
			501		
	510				
552	552	552			C–C–C deformation
	584				
	595				
			618		Phe
	627				C–C twisting, Phe
		657			Tyr
	660				C–S stretch
			670		Val
	678				
		683			
	695			694	
702					
			719		Adenine;
	724				Peptidoglycan
733	732	731	730		Adenine; Peptidoglycan
	757				Trp
765	**765**	**764**	**766**	**764**	C–C galactose
	772	773		772	
779			779		
		782			
785	786			785	Cytosine, Uracil (ring stretching)
804	**805**	**806**	**808**	**804**	C–C deformation/O–C–O wagging/C–H vibrations with C–OH
819			820	820	Tyr
837	838				Tyr

Table 2. *Cont.*

Control BHI	*Listeria*	*S. aureus*	*E. coli*	*Salmonella*	Attribution
844					
	852			852	Tyr
				863	C–C stretching, C–O–C 1,4 glycosidic ring
877					C–O–C stretching/Trp
	885	885	884	884	C–O–C stretching/Trp
			895		
		901		904	Teicuronic acid Gram-positive, Adenine
913					
926	926				Saccharides
943	**944**	**940**	**939**	**940**	Saccharides, Prot/skel C–C, C–C–N stretching, N–C stretching
					C–C amide/protein, N–C stretching
	968				C–CH deformation
975					
	1000				Phe
1030	1030				C–O exocycling stretching, Phe
1067	1066			1067	C–O exocycling stretching, side chain Lys, Asp, Glu, C–C–C stretching
1083	1084	1084			C–OH deformation/C–C–O stretching
			1087	1086	Nucleic acids (PO_2 simetrical stretching), DNA phosphate backbone
				1119	Trp
1131	1131				Phe
	1154				C–C, C–N protein stretching, CH_3 def
	1173				C–H wagging of Tyr, Guanine, Cytosine, fatty acids, CH_3 deformation
1175				1175	Tyr–Phe
		1177			
1205				1206	Tyr–Phe
	1209	1209			Tyr–Phe
1229	1230				C–H stretching, Haemoglobin, Amide III
	1244			1244	Amide III
1250					Amide
	1285				Amide III, CH_2 twisting
	1295	1297			CH_2 fatty acid deformation, cytosine
1308					
	1311			1310	
				1320	CH_2 deformation
		1324			
	1326		1326		
1332	**1333**	**1333**	**1335**	**1333**	Amide III vibrations, Trp, Cα-H vibrations, CH deformation
				1341	
		1344	1344		
1351			1352	1350	CH_2 wagging
			1357		
			1369		
				1492	Lipids, CH deformation of fatty acids, CH_2 deformation
1573					DNA/RNA, Adenine, Guanine, ring stretching
	1582				Guanine, Adenine, ring stretching, Phe, Trp
1593	1592				
1600					Phe
	1609			1609	Phe, Tyr
1627					Trp, Tyr
		1629			
	1635				Thymine, Guanine

Hence, we propose a detection method employing two culture steps using relatively low-cost media: first culture step—colony isolation in BHI agar (24–36 h), and second axenic culture step—bacterial cell growth in BHI broth. The culture obtained in the second step is used for Raman measurements after 18–24 h growth. The proposed method would take up to 60 h of detection time, with minimal sample preparation, using low reagent levels and reduced bench-work time with an accuracy >0.90. Some of the limitations of this technique are that it depends on the isolation step in the agar medium and its subculture in the broth medium for monoculture identification. Further experiments are being carried out to build a comprehensive library of bacterial spectra to explore further the potential of Raman to identify other bacterial species and among strains of the same species.

5. Conclusions

In this study, we demonstrated the capability to differentiate monocultures accurately and to correctly detect *E. coli*, *L. monocytogenes*, *S. enterica*, and *S. aureus* after 24 h of growth with an accuracy of 0.93 ($\pm$0.20) using a low-cost portable Raman handheld device equipped with Orbital Raster Scan technology combined with PCA and SVM as a classifier. To our knowledge, this is the first report using a Raman handheld device with ORS technology for the detection of suspended cells on media broth using minimal sample preparation, i.e., 1 mL of 24 h growth cell suspension, making it a very convenient technique for a large volume of samples achieving high accuracy in a shorter time compared to conventional culture methods, and with lower cost compared to other Raman techniques such as SERS that require a substantial initial capital investment. Therefore, this detection method could be viable in low-resource settings, such as temporary laboratories set up in remote areas or temporary emergency units by minimally trained personnel.

References

1. Focker, M.; van der Fels-Klerx, H.J. Economics Applied to Food Safety. *Curr. Opin. Food Sci.* **2020**, *36*, 18–23. [CrossRef]
2. Barba, F.J.; Koubaa, M.; do Prado-Silva, L.; Orlien, V.; Sant'Ana, A.d.S. Mild Processing Applied to the Inactivation of the Main Foodborne Bacterial Pathogens: A Review. *Trends Food Sci. Technol.* **2017**, *66*, 20–35. [CrossRef]
3. Adams, M.R.; Moss, M.O.; McClure, P.J. *Food Microbiology*, 4th ed.; Royal Society of Chemistry, Ed.; Royal Society of Chemistry: London, UK, 2016; ISBN 978-1-84973-960-3.
4. Majowicz, S.E.; Musto, J.; Scallan, E.; Angulo, F.J.; Kirk, M.; O'Brien, S.J.; Jones, T.F.; Fazil, A.; Hoekstra, R.M. The Global Burden of Nontyphoidal Salmonella Gastroenteritis. *Clin. Infect. Dis.* **2010**, *50*, 882–889. [CrossRef]
5. Koutsoumanis, K.; Allende, A.; Alvarez-Ordóñez, A.; Bolton, D.; Bover-Cid, S.; Chemaly, M.; de Cesare, A.; Herman, L.; Hilbert, F.; Lindqvist, R.; et al. Salmonella Control in Poultry Flocks and Its Public Health Impact. *EFSA J.* **2019**, *17*, e05596. [PubMed]
6. European Food Safety Authority and European Centre for Disease Prevention and Control (EFSA and ECDC). EFSA and The European Union Summary Report on Trends and Sources of Zoonoses, Zoonotic Agents and Food-Borne Outbreaks in 2017. *EFSA J.* **2018**, *16*, e05500. [CrossRef]

7. Witkowska, E.; Korsak, D.; Kowalska, A.; Księżopolska-Gocalska, M.; Niedziółka-Jönsson, J.; Roźniecka, E.; Michałowicz, W.; Albrycht, P.; Podrażka, M.; Hołyst, R.; et al. Surface-Enhanced Raman Spectroscopy Introduced into the International Standard Organization (ISO) Regulations as an Alternative Method for Detection and Identification of Pathogens in the Food Industry. *Anal. Bioanal. Chem.* **2017**, *409*, 1555–1567. [CrossRef] [PubMed]

8. Knabl, L.; Huber, S.; Lass-Fl€, C.; Fuchs, S.; Fuchs, S. Comparison of Novel Approaches for Expedited Pathogen Identification and Antimicrobial Susceptibility Testing against Routine Blood Culture Diagnostics. *Lett. Appl. Microbiol.* **2021**, *73*, 2–8. [CrossRef]

9. Deidda, R.; Sacre, P.Y.; Clavaud, M.; Coïc, L.; Avohou, H.; Hubert, P.; Ziemons, E. Vibrational Spectroscopy in Analysis of Pharmaceuticals: Critical Review of Innovative Portable and Handheld NIR and Raman Spectrophotometers. *TrAC-Trends Anal. Chem.* **2019**, *114*, 251–259. [CrossRef]

10. Lorenz, B.; Wichmann, C.; Stöckel, S.; Rösch, P.; Popp, J. Special Issue: From One to Many Cultivation-Free Raman Spectroscopic Investigations of Bacteria. *Trends Microbiol.* **2017**, *25*, 413–424. [CrossRef]

11. Chao, Y.; Zhang, T. Surface-Enhanced Raman Scattering (SERS) Revealing Chemical Variation during Biofilm Formation: From Initial Attachment to Mature Biofilm. *Anal. Bioanal. Chem.* **2012**, *404*, 1465–1475. [CrossRef]

12. Cho, I.H.; Bhandari, P.; Patel, P.; Irudayaraj, J. Membrane Filter-Assisted Surface Enhanced Raman Spectroscopy for the Rapid Detection of E. Coli O157:H7 in Ground Beef. *Biosens. Bioelectron.* **2015**, *64*, 171–176. [CrossRef]

13. Yilmaz, A.G.; Temiz, H.T.; Acar Soykut, E.; Halkman, K.; Boyaci, I.H. Rapid Identification of Pseudomonas Aeruginosa and Pseudomonas Fluorescens Using Raman Spectroscopy. *J. Food Saf.* **2015**, *35*, 501–508. [CrossRef]

14. Zong, C.; Xu, M.; Xu, L.-J.; Wei, T.; Ma, X.; Zheng, X.-S.; Hu, R.; Ren, B. Surface-Enhanced Raman Spectroscopy for Bioanalysis: Reliability and Challenges. *Chem. Rev.* **2018**, *118*, 4946–4980. [CrossRef]

15. Ho, C.S.; Jean, N.; Hogan, C.A.; Blackmon, L.; Jeffrey, S.S.; Holodniy, M.; Banaei, N.; Saleh, A.A.E.; Ermon, S.; Dionne, J. Rapid Identification of Pathogenic Bacteria Using Raman Spectroscopy and Deep Learning. *Nat. Commun.* **2019**, *10*, 4927. [CrossRef]

16. García-Timermans, C.; Rubbens, P.; Kerckhof, F.M.; Buysschaert, B.; Khalenkow, D.; Waegeman, W.; Skirtach, A.G.; Boon, N. Label-Free Raman Characterization of Bacteria Calls for Standardized Procedures. *J. Microbiol. Methods* **2018**, *151*, 69–75. [CrossRef]

17. Farber, C.; Kurouski, D. Detection and Identification of Plant Pathogens on Maize Kernels with a Hand-Held Raman Spectrometer. *Anal. Chem.* **2018**, *90*, 3009–3012. [CrossRef]

18. Lemma, T.; Saliniemi, A.; Hynninen, V.; Hytönen, V.P.; Toppari, J.J. SERS Detection of Cell Surface and Intracellular Components of Microorganisms Using Nano-Aggregated Ag Substrate. *Vib. Spectrosc.* **2016**, *83*, 36–45. [CrossRef]

19. Premasiri, W.R.; Gebregziabher, Y.; Ziegler, L.D. On the Difference between Surface-Enhanced Raman Scattering (SERS) Spectra of Cell Growth Media and Whole Bacterial Cells. *Appl. Spectrosc.* **2011**, *65*, 493–499. [CrossRef]

20. Berezin, S.; Aviv, Y.; Aviv, H.; Goldberg, E.; Tischler, Y.R. Replacing a Century Old Technique—Modern Spectroscopy Can Supplant Gram Staining. *Sci. Rep.* **2017**, *7*, 3810. [CrossRef]

21. Zeiri, L.; Bronk, B.V.; Shabtai, Y.; Eichler, J.; Efrim, S. Surface-Enhanced Raman Spectroscopy as a Tool for Probing Specific Biochemical Components in Bacteria. *Appl. Spectrosc.* **2004**, *58*, 33–40. [CrossRef]

22. Pahlow, S.; Meisel, S.; Cialla-May, D.; Weber, K.; Rösch, P.; Popp, J. Isolation and Identification of Bacteria by Means of Raman Spectroscopy. *Adv. Drug Deliv. Rev.* **2015**, *89*, 105–120. [CrossRef]

23. Senes, A.; Ubarretxena-Belandia, I.; Engelman, D.M. The Cα-H···O Hydrogen Bond: A Determinant of Stability and Specificity in Transmembrane Helix Interactions. *Proc. Natl. Acad. Sci. USA* **2001**, *98*, 9056–9061. [CrossRef]

24. Geravand, A.; Hashemi Nezhad, S.M. Simulation Study of the Orbital Raster Scan (ORS) on the Raman Spectroscopy. *Optik* **2019**, *178*, 83–89. [CrossRef]

25. Notingher, I.; Verrier, S.; Romanska, H.; Bishop, A.E.; Polak, J.M.; Hench, L.L. *In Situ Characterisation of Living Cells by Raman Spectroscopy*; IOS Press: Amsterdam, The Netherlands, 2002; Volume 16.

26. Ravindranath, S.P.; Wang, Y.; Irudayaraj, J. SERS Driven Cross-Platform Based Multiplex Pathogen Detection. *Sens. Actuators B Chem.* **2011**, *152*, 183–190. [CrossRef]

27. Duan, N.; Yan, Y.; Wu, S.; Wang, Z. Vibrio Parahaemolyticus Detection Aptasensor Using Surface-Enhanced Raman Scattering. *Food Control* **2016**, *63*, 122–127. [CrossRef]

28. Jarvis, R.M.; Brooker, A.; Goodacre, R. Surface-Enhanced Raman Scattering for the Rapid Discrimination of Bacteria. *Faraday Discuss.* **2005**, *132*, 281–292. [CrossRef]

29. Li Vigni, M.; Durante, C.; Michelini, S.; Nocetti, M.; Cocchi, M. Preliminary Assessment of Parmigiano Reggiano Authenticity by Handheld Raman Spectroscopy. *Foods* **2020**, *9*, 1563. [CrossRef]

30. Li, R.; Dhankhar, D.; Chen, J.; Krishnamoorthi, A.; Cesario, T.C.; Rentzepis, P.M. Identification of Live and Dead Bacteria: A Raman Spectroscopic Study. *IEEE Access* **2019**, *7*, 23549–23559. [CrossRef]

31. Luo, B.S.; Lin, M. A Portable Raman System for the Identification of Foodborne Pathogen Bacteria. *J. Rapid Methods Autom. Microbiol.* **2008**, *16*, 238–255. [CrossRef]

32. Maquelin, K.; Kirschner, C.; Choo-Smith, L.P.; van den Braak, N.; Endtz, H.P.; Naumann, D.; Puppels, G.J. Identification of Medically Relevant Microorganisms by Vibrational Spectroscopy. *J. Microbiol. Methods* **2002**, *51*, 255–271. [CrossRef]

33. Münchberg, U.; Rösch, P.; Bauer, M.; Popp, J. Raman Spectroscopic Identification of Single Bacterial Cells under Antibiotic Influence. *Anal. Bioanal. Chem.* **2014**, *406*, 3041–3050. [CrossRef] [PubMed]

34. Santana De Siqueira, F.; Hector, O.; Giana, E.; Silveira, L. Discrimination of Selected Species of Pathogenic Bacteria Using Near-Infrared Raman Spectroscopy and Principal Components Analysis. *J. Biomed. Opt.* **2012**, *17*, 107004. [CrossRef] [PubMed]

35. Vohník, S.; Hanson, C.; Tuma, R.; Fuchs, J.A.; Woodward, C.; Thomas, G. Conformation, Stability, and Active-Site Cysteine Titrations of Escherichia Coli D26A Thioredoxin Probed by Raman Spectroscopy. *Protein Sci.* **1998**, *7*, 193–200. [CrossRef] [PubMed]